Side-sensitive modified group runs charts with and without measurement errors for monitoring the coefficient of variation

Sajal Saha, Michael B C Khoo, Philippe Castagliola, Abdul Haq

Side-sensitive modified group runs charts with and without measurement errors for monitoring the coefficient of variation

Sajal Saha

Department of Mathematics,

International University of Business Agriculture and Technology, Dhaka, Bangladesh

sajal.saha@iubat.edu

Michael B. C. Khoo (Corresponding Author)

School of Mathematical Sciences,

Universiti Sains Malaysia, 11800 Penang, Malaysia

mkbc@usm.my

Philippe Castagliola

Université de Nantes & LS2N UMR CNRS 6004, Nantes, France

philippe.castagliola@univ-nantes.fr

Abdul Haq

Department of Statistics, Quaid-i-Azam University, Islamabad, Pakistan

aaabdulhaq@yahoo.com

Side-sensitive modified group runs charts with and without measurement errors for monitoring the coefficient of variation

Abstract

The coefficient of variation (CV) is used in process monitoring when the process mean and standard deviation are proportional to each other. In this work, a side-sensitive modified group runs CV (SSMGR CV) chart is proposed for monitoring the process CV. The run length performance of the SSMGR CV chart is compared with those of the existing CV charts in terms of the average and standard deviation of the run length criteria. The SSMGR CV chart is found to outperform the existing CV charts. In addition, the run length performance of the SSMGR CV chart is also evaluated in the presence of measurement errors, as these errors are not only unavoidable in practice but they also affect the sensitivity of a control chart in detecting an out-of-control situation. The results obtained show that the *accuracy* and *precision* errors affect the performance of the SSMGR CV chart in detecting an out-of-control situation.

Keywords: Coefficient of variation; side-sensitive modified group runs (SSMGR); average run length; standard deviation of the run length; measurement error

1. Introduction

A control chart is the most important tool in Statistical Process Control (SPC) to detect process shifts, in order to reduce process variability in manufacturing or service industries. The $\bar{X}$ and S charts are commonly used to ensure that the process mean and standard deviation, respectively, remain in-control at their nominal values, μ_0 and σ_0, respectively. However, there are many

processes where the mean is not constant and/or the standard deviation is a function of the mean. In such processes, the process mean and standard deviation may change but as long as the ratio of the process standard deviation to the mean is constant, the said processes are assumed to be in-control. For this type of processes, the conventional $\bar{X}$ and S charts are no longer suitable in process monitoring because these two charts monitor the process mean and process standard deviation separately and neither of them monitors the ratio of the process standard deviation to the mean. Instead, the CV (denoted as $\gamma = \sigma / \mu$), which is a ratio of the process standard deviation to the mean, is a suitable quality characteristic in process monitoring for the aforesaid type of processes.

Kang et al [1] introduced the Shewhart CV chart and showed that this chart is an effective quality control tool for quality improvement, when neither the process mean nor the process variance is constant. However, the Shewhart CV chart is not efficient in detecting small and moderate CV shifts. To improve the efficiency of the Shewhart CV chart, Hong et al [2] proposed a two-sided exponentially weighted moving average (EWMA) CV chart that is efficient in detecting small and moderate CV shifts. Later, Castagliola et al [3] presented a one-sided EWMA CV chart and showed that the new chart is more efficient than the two-sided EWMA CV chart of Hong et al [2] in detecting CV shifts. To incorporate adaptive features into the Shewhart CV chart, Castagliola et al [4] and Castagliola et al [5] proposed the variable sampling interval CV and variable sample size CV charts, respectively, where they found that these CV charts outperform the Shewhart CV chart.

On similar lines, Calzada and Scariano [6] proposed the synthetic CV chart and compared its performance with the Shewhart CV and one-sided EWMA CV charts. The synthetic CV chart was found to outperform the Shewhart CV chart but the EWMA CV chart is superior to the synthetic CV chart in detecting small CV shifts. You et al [7] studied the performance of the side-sensitive

group runs (SSGR) chart for monitoring the CV and compared its performance with the Shewhart CV, synthetic CV and EWMA CV charts. The findings showed that the SSGR CV chart surpasses the basic CV and synthetic CV charts. Noor-ul-Amin et al [8] proposed a blended control chart with and without auxiliary information for a simultaneous monitoring of the process mean and CV and found that the sensitivity of the proposed chart is enhanced by incorporating auxiliary information. An EWMA chart for multivariate CV was introduced by Giner-Bosch [9] and it was shown that the aforementioned chart outperforms its existing counterparts. For recent research works on the CV charts, readers may refer to Teoh et al, [10] Khaw et al, [11] Yeong et al, [12] Yeong et al [13] and Chew et al [14]

Numerous group runs (GR) schemes were introduced to enhance the sensitivity of the synthetic $\bar{X}$ chart proposed by Wu and Spedding [15]. This paragraph discusses the GR schemes that exist in the literature. Gadre and Rattihalli [16] introduced the GR $\bar{X}$ chart by combining the $\bar{X}$ chart with the conforming run length (CRL) chart. The CRL sub-chart is a type of lower-sided chart that is used to determine whether the process being monitored is in-control or otherwise. The GR $\bar{X}$ chart signals an out-of-control if $\mathrm{CRL}_1 < L$ or both CRL_r and CRL_{r+1} (for r >1) are less than L, where L is the lower limit of the CRL sub-chart (of the GR $\bar{X}$ chart). Here, CRL_r represents the number of conforming samples, inspected between the $(r-1)^{\text{th}}$ and r^{th} non-conforming samples, including the r^{th} non-conforming sample. It was found that the GR $\bar{X}$ chart outperforms the synthetic $\bar{X}$ and Shewhart $\bar{X}$ charts.

Gadre and Rattihalli [17] extended the GR $\bar{X}$ charting concept to the modified GR (MGR) $\bar{X}$ chart by adding an additional lower limit to the CRL sub-chart (of the MGR $\bar{X}$ chart). The MGR $\bar{X}$ chart signals an out-of-control if $\mathrm{CRL}_1 < L_2$ or for some r (> 1), $\mathrm{CRL}_r < L_1$ and $\mathrm{CRL}_{r+1} < L_2$.

Here, L_1 and L_2 are the lower limits of the CRL sub-chart (of the MGR $\bar{X}$ chart). Note that if $L_1 = L_2 = L$, the MGR $\bar{X}$ chart reduces to the GR $\bar{X}$ chart. On similar lines, by adding the side-sensitive feature to the GR $\bar{X}$ and MGR $\bar{X}$ charts, Gadre and Rattihalli [18] and Gadre et al [19] introduced the side-sensitive GR (SSGR) $\bar{X}$ and the side-sensitive MGR (SSMGR) $\bar{X}$ charts, respectively. Both the SSGR and SSMGR charts signal an out-of-control if the sample means $\left(\bar{X}\right)$ corresponding to the two successive CRLs that contribute to the out-of-control signal plot on the same side of the target value on the $\bar{X}$ sub-chart (of the respective SSGR $\bar{X}$ and SSMGR $\bar{X}$ charts). In terms of the effectiveness of the charts in detecting process mean shifts, Gadre et al [19] showed that the SSMGR $\bar{X}$ chart outperforms the Shewhart $\bar{X}$, synthetic $\bar{X}$, GR $\bar{X}$, MGR $\bar{X}$ and SSGR $\bar{X}$ charts. More recent extensions on the GR type charts include You et al, [20] Khoo et al, [21] Chong et al, [22] Saha et al, [23] Chong et al, [24] Mim et al, [25] and Gadre and Kakade. [26]

Note that in the Shewhart $\bar{X}$ chart, a decision about the state of the process being monitored is dependent on where the sample mean plots on the chart. If the sample mean plots beyond the limits of the $\bar{X}$ chart, the process is out-of-control, otherwise, it is in-control. On the other hand, for the $\bar{X}$ sub-chart of a GR $\bar{X}$ type chart (such as the MGR $\bar{X}$, SSGR $\bar{X}$ and SSMGR $\bar{X}$ charts), a sample mean that plots beyond (within) the limits of the $\bar{X}$ sub-chart is considered as a non-conforming (conforming) sample, instead of an out-of-control (in-control) sample. A decision as to whether a process being monitored using a GR $\bar{X}$ type chart is in-control or out-of-control is made according to the outcome given by the conforming run length (CRL) sub-chart, where the points on the CRL sub-chart are plotted based on the information provided by the $\bar{X}$ sub-chart.

Control charts are usually designed with the assumption that the measurements on the quality characteristics are obtained without any measurement error. However, in usual practice,

measurement errors often exist and affect the performances of the control charts. Linna and Woodall [27] introduced the linear covariate error model to investigate the effect of measurement errors on the $\bar{X}$ and S^2 charts, and they recommended taking multiple measurements per item in order to reduce the effect of measurement errors. Using the same covariate error model of Linna and Woodall, [27] Linna et al [28] studied the performance of multivariate control charts in the presence of measurement errors, where they found that the ability of the control charts to detect shifts in one direction is better than in the other direction due to the loss of the directional invariance property. Costa and Castagliola [29] studied the performance of the $\bar{X}$ chart in the presence of measurement errors and autocorrelated data, and they showed that the effect of autocorrelation can be reduced by taking samples with non-neighboring items. The effects of measurement errors on the two one-sided Shewhart charts for monitoring the ratio of two normal variables were investigated by Nguyen and Tran [30], where it was found that the two one-sided charts are more advantageous than the two-sided Shewhart chart for the ratio. Additionally, Tran et al [31] proposed the synthetic median chart to improve the efficiency of the Shewhart median chart in detecting small and moderate mean shifts, followed by conducting an investigation of the effects of measurement errors on the synthetic median chart. Additional researches that investigated the effect of measurement errors on different types of control charts were made by Maravelakis, [32] Hu et al, [33] Noorossana and Zerehsaz, [34] Tran et al, [35] Tran et al, [36] Yeong et al [37] and Tran et al. [38]

Due to the sensitivity of the SSMGR chart towards process shifts and the widespread use of CV in real life, the SSMGR chart for monitoring the process CV (called the SSMGR CV chart) is developed in this research. The charting statistic, optimal design and implementation procedure of the proposed chart are presented. The SSMGR CV chart is compared with the existing EWMA CV, run sum (RS) CV and SSGR CV charts, in terms of the average run length (ARL) and standard

deviation of the run length (SDRL) criteria, where the results show that the SSMGR CV chart generally outperforms the existing charts. Additionally, the detection ability of the SSMGR CV chart in the presence of measurement errors (called the SSMGR CV-ME chart) is also investigated in detail. The charting statistic, optimal design and implementation procedure of the SSMGR CV-ME chart are also discussed. Moreover, a step-by-step implementation procedure of the SSMGR CV-ME chart using a real industrial dataset is given to explain the working of the proposed chart in usual practice.

The rest of this paper is organized as follows: Section 2 presents the basic properties of the CV. The SSMGR CV chart is presented in Section 3. Section 4 explains the linear covariate error model for the CV. Section 5 discusses the SSMGR CV-ME chart. The optimal design procedure to minimize the out-of-control value of ARL for the SSMGR CV and SSMGR CV-ME charts are discussed in Section 6. The performances of the SSMGR CV and SSMGR CV-ME charts are evaluated in Section 7. Section 8 shows the implementation of the SSMGR CV-ME chart using a real dataset. Lastly, conclusions are drawn in Section 9.

2. Basic properties of CV

Let X be a random variable having mean μ and standard deviation σ, then the CV of X is

$$\gamma = \frac{\sigma}{\mu}. \tag{1}$$

Let $\{X_1, X_2, ..., X_n\}$ be a random sample of size n from the normal $N(\mu, \sigma^2)$ distribution, i.e. $X_i \sim N(\mu, \sigma^2)$ for $i = 1, 2, \ldots, n$. The sample mean $\bar{X}$ and sample standard deviation S computed from this sample are

$$\bar{X} = \frac{1}{n}\sum_{i=1}^{n} X_i \tag{2}$$

and

$$S = \sqrt{\frac{1}{n-1}\sum_{i=1}^{n}\left(X_i - \bar{X}\right)^2}\,, \tag{3}$$

respectively. Based on $\bar{X}$ and S, the sample CV $\left(\hat{\gamma}\right)$ is computed as

$$\hat{\gamma} = \frac{S}{\bar{X}}. \tag{4}$$

In the literature, the probability distribution of $\hat{\gamma}$ has been investigated by numerous researchers, such as McKay, [39] Iglewicz et al [40] and Iglewicz and Myers, [41] to name a few. Iglewicz et al [40] showed that $\sqrt{n}/\hat{\gamma}$ follows the non-central t distribution with $n-1$ degrees of freedom with the non-centrality parameter $\sqrt{n}/\gamma$. Following this result, Castagliola et al [3] showed that the cumulative distribution function (cdf) of $\hat{\gamma}$ is

$$F_{\hat{\gamma}}\left(x \mid n,\gamma\right) = 1 - F_t\left(\frac{\sqrt{n}}{x}\middle| n-1, \frac{\sqrt{n}}{\gamma}\right), \tag{5}$$

where $F_t\left(\cdot \middle| n-1, \frac{\sqrt{n}}{\gamma}\right)$ is the cdf of the non-central t distribution with $n-1$ degrees of freedom and non-centrality parameter $\sqrt{n}/\gamma$. The inverse cdf of $\hat{\gamma}$ is given by (Castagliola et al [3])

$$F_{\hat{\gamma}}^{-1}\left(x\middle|n,\gamma\right) = \frac{\sqrt{n}}{F_t^{-1}\left(1-x\middle|n-1,\frac{\sqrt{n}}{\gamma}\right)}. \tag{6}$$

3. The SSMGR CV chart

The SSMGR CV chart consists of the CV sub-chart and an extended version of the CRL sub-chart. The upper and lower control limits (UCL and LCL) of the CV sub-chart of the SSMGR CV chart are

$$\text{UCL} = F_{\hat{\gamma}}^{-1}\left(1-\frac{k}{2}\middle| n,\gamma_0\right) \tag{7a}$$

and

$$\text{LCL} = F_{\hat{\gamma}}^{-1}\left(\frac{k}{2}\middle| n,\gamma_0\right), \tag{7b}$$

respectively, where k is the limits' constant that is used to adjust the limits in order to attain the desired in-control performance of the chart, while γ_0 is the target value of the process CV.

If the charting statistic of the SSMGR CV chart, i.e. $\hat{\gamma}$, computed using Equation (4), falls beyond the UCL/LCL limits, the current sample CV is declared as non-conforming. Let CRL_r represent the number of conforming $\hat{\gamma}$ samples, inspected between the $(r-1)^{\text{th}}$ and r^{th} non-conforming $\hat{\gamma}$ samples, including the r^{th} non-conforming $\hat{\gamma}$ sample. The implementation of the SSMGR CV chart is as follows:

Step 1. Take a sample of size n and compute $\hat{\gamma}$.

Step 2. If $\hat{\gamma} \in [\text{LCL},\text{UCL}]$, the sample is classified as conforming, then return to Step 1. Otherwise, the sample is non-conforming and proceed to Step 3.

Step 3. Compute CRL_r, for r = 1, 2, ... If $\text{CRL}_1 \le C_2$ or for $r > 1$, $\text{CRL}_r \le C_1$ and $\text{CRL}_{r+1} \le C_2$, declare the process as out-of-control, where C_f (for f = 1, 2) are the lower limits of the CRL sub-chart (of the SSMGR CV chart). Otherwise, return to Step 1.

There are three design parameters of the SSMGR CV chart, i.e. k, C_1 and C_2.

Let P denote the probability of $\hat{\gamma}$ falling beyond the UCL/LCL limits of the SSMGR CV chart. Then

$$P = 1 - \Pr\left(\text{LCL} \le \hat{\gamma} \le \text{UCL}\right)$$

$$= 1 - F_{\hat{\gamma}}\left(\text{UCL} \middle| n, \gamma\right) + F_{\hat{\gamma}}\left(\text{LCL} \middle| n, \gamma\right). \tag{8}$$

As the SSMGR CV chart considers the side-sensitive feature, it is necessary to consider the conditional probability

$$\alpha = \Pr\left(\hat{\gamma} > \text{UCL} \middle| \hat{\gamma} \notin \left[\text{LCL}, \text{UCL}\right]\right)$$

$$= \frac{\Pr\left(\hat{\gamma} > \text{UCL} \cap \hat{\gamma} \notin \left[\text{LCL}, \text{UCL}\right]\right)}{\Pr\left(\hat{\gamma} \notin \left[\text{LCL}, \text{UCL}\right]\right)}$$

$$= \frac{1 - F_{\hat{\gamma}}\left(\text{UCL} \middle| n, \gamma\right)}{P}. \tag{9}$$

The Markov chain approach, similar to that in Gadre et al [19], is used to compute the ARL values of the SSMGR CV chart. The description of the Markov chain states of the samples are given in Table 1. Note that the states of the Markov chain model for the SSMGR CV chart depend on the values of the positive integers, say C_1 and C_2. As an example, Table 2 shows the complete states of the Markov chain model for the SSMGR CV chart when $C_1 = C_2 = 3$. The following steps explain the procedure to obtain the states of the Markov chain model for the SSMGR CV chart:

1. A sequence starting with $\underline{\bar{G}}$ (or $\bar{G}$ or $\underline{G}$), followed by a maximum of $\left(C_2 - 1\right)$ $\tilde{0}$'s. There are $3C_2$ such states (see states 1 – 3, 5, 6, 8 – 11 in Table 2).
2. A sequence of C_2 $\tilde{0}$'s. There is only one state of this type (see state 4 in Table 2).

3. A sequence starting with G (or $\bar{H}$ or $\underline{H}$), followed by a maximum of $(C_1 - 1)$ 0's. There are $3C_1$ such states (see states 12 – 20 in Table 2).

4. A sequence of C_1 0's. Only one state of this type is available (see state 7 in Table 2).

5. Signal (see state 21 in Table 2).

The total number of states, including the absorbing state is $3C_2 + 1 + 3C_1 + 1 + 1 = 3(C_2 + C_1 + 1)$. Table 2 presents the 21 different states of the Markov chain model for the SSMGR CV chart, based on $C_1 = 3$ and $C_2 = 3$. In Table 2, states 1 – 20 are non-absorbing states while state 21 is an absorbing state.

Let $\boldsymbol{R}$ be the transition probability matrix (tpm) of the Markov chain model for the SSMGR CV chart without the absorbing state. Let $T = 1 - P$ and $S = P$, then the (g,h)th entry of matrix $\boldsymbol{R}$ is obtained as follows (Gadre et al [19]):

$$R_{g,h} = \begin{cases} T \text{ if the gth state leads to the } h\text{th state and the } h\text{th state corresponds to the sequence ending with 0 (or } \tilde{0}). \\ S \text{ if the gth state leads to the } h\text{th state and the } h\text{th state corresponds to the sequence ending with } G. \\ \alpha S \text{ if the gth state leads to the } h\text{th state and the } h\text{th state corresponds to the sequence ending with } \overline{G} \text{ (or } \overline{H}). \\ (1 - \alpha)S \text{ if the gth state leads to the } h\text{th state and the } h\text{th state corresponds to the sequence ending with } \underline{G} \text{ (or } \underline{H}). \\ 0 \text{ otherwise.} \end{cases}$$

In general, the tpm $\boldsymbol{R}$ of the SSMGR CV chart is a square matrix with a dimension of $(3(C_1 + C_2) + 2) \times (3(C_1 + C_2) + 2)$. As an example, Table 3 presents the entries of $\boldsymbol{R}$ corresponding to the values $C_1 = C_2 = 3$. The ARL and SDRL of the SSMGR CV chart, for a shift size τ, are computed as

$$\mathrm{ARL}(\tau) = v_1 \tag{10}$$

and

$$\mathrm{SDRL}(\tau) = \sqrt{v_2 - v_1^2 + v_1}\,, \tag{11}$$

respectively, where

$$v_1 = \boldsymbol{q}^T \left(\boldsymbol{I} - \boldsymbol{R}\right)^{-1} \mathbf{1} \tag{12}$$

and

$$v_2 = 2\boldsymbol{q}^T \left(\boldsymbol{I} - \boldsymbol{R}\right)^{-2} \boldsymbol{R} \cdot \mathbf{1}\,. \tag{13}$$

Here, $\boldsymbol{q}^T = (1, 0, 0, \ldots, 0)$ is the initial probability vector and its dimension is $\left(3\left(C_1 + C_2\right) + 2\right) \times 1$, $\boldsymbol{I}$ is the $\left(3\left(C_1 + C_2\right) + 2\right) \times \left(3\left(C_1 + C_2\right) + 2\right)$ identity matrix and $\mathbf{1}$ is a $\left(3\left(C_1 + C_2\right) + 2\right)1$ column vector whose entries are all ones.

Let γ_1 be the value of the out-of-control CV and $\tau = \gamma_1/\gamma_0$ be the standardized CV shift from γ_0 to γ_1. By definition, an upward shift in the process CV occurs when $\tau > 1$ and a downward shift in the process CV happens when $\tau < 1$. The process CV is said to be in the in-control state when $\tau = 1$.

4. Linear covariate error model for the CV

Let $\left\{X_{i,1}, X_{i,2}, \ldots, X_{i,n}\right\}$ denote the ith sample of quality characteristics, where $X_{i,j} \sim N\left(\mu_0 + a\sigma_0,\ b^2\sigma_0^2\right)$, for $j = 1, 2, \ldots, n$ and $n > 1$. Here, μ_0 and σ_0 are the nominal mean and standard deviation, respectively. In addition, a and b denote the sizes of the standardized mean and standard deviation shifts, respectively. The process has shifted when $a \neq 0$ or/and $b \neq 1$. It is

assumed that the quality characteristic $X_{i,j}$ cannot be observed directly but can only be obtained from the results $\left\{X^*_{i,j,1}, X^*_{i,j,2}, ..., X^*_{i,j,m}\right\}$ of a set of $m \geq 1$ characteristics, where each $X^*_{i,j,k}$ satisfies the following linear covariate error model (Tran et al [38]):

$$X^*_{i,j,k} = A + BX_{i,j} + \varepsilon_{i,j,k}. \tag{14}$$

Here, *A* and *B* are two known constants and $\varepsilon_{i,j,k}$ is a normal $N\left(0,\ \sigma_M^2\right)$ random error term due to measurement inaccuracy, which is supposed to be independent of $X_{i,j}$.

For sample *i* (*i* = 1, 2, …), there exists $m \times n$ observations $X^*_{i,j,k}$, for *j* = 1, 2, …, *n* and *k* = 1, 2, …, *m*. Then, the mean $\bar{X}^*_{i,j}$ of the characteristics $\left\{X^*_{i,j,1}, X^*_{i,j,2}, ..., X^*_{i,j,m}\right\}$ is computed as (Tran et al [38])

$$\begin{aligned}\bar{X}^*_{i,j} &= \frac{1}{m}\sum_{k=1}^{m} X^*_{i,j,k} \\ &= \frac{1}{m}\sum_{k=1}^{m}\left(A + BX_{i,j} + \varepsilon_{i,j,k}\right) \\ &= A + BX_{i,j} + \frac{1}{m}\sum_{k=1}^{m}\varepsilon_{i,j,k}\ .\end{aligned} \tag{15}$$

The mean and standard deviation of $\bar{X}^*_{i,j}$ are (Tran et al [38])

$$\mu^* = A + B\left(\mu_0 + a\sigma_0\right) \tag{16}$$

and

$$\sigma^* = \sqrt{B^2 b^2 \sigma_0^2 + \frac{\sigma_M^2}{m}}, \tag{17}$$

respectively. Consequently, the CV of the measured characteristic $\bar{X}^*_{i,j}$ is obtained as

$$\gamma^* = \frac{\sigma^*}{\mu^*} = \frac{\sqrt{B^2 b^2 \sigma_0^2 + \sigma_M^2 / m}}{A + B\left(\mu_0 + a\sigma_0\right)}$$

$$= \frac{\gamma_0 \sqrt{B^2 b^2 + \eta^2 / m}}{\theta + B\left(1 + a\gamma_0\right)}, \tag{18}$$

where $\eta = \frac{\sigma_M}{\sigma_0}$, $\theta = \frac{A}{\mu_0}$ and $\gamma_0 = \frac{\sigma_0}{\mu_0}$. Here, η is called the precision error ratio, θ is the accuracy error and γ_0 is the nominal value of the population CV. Note that γ^* in Equation (18) no longer depends on parameter *A*.

Let $\bar{\bar{X}}_i^*$ and S_i^* be the sample mean and sample standard deviation of $\left\{\bar{X}_{i,1}^*, \bar{X}_{i,2}^*, ..., \bar{X}_{i,n}^*\right\}$. Then (Tran et al [38])

$$\bar{\bar{X}}_i^* = \frac{1}{n}\sum_{j=1}^{n} \bar{X}_{i,j}^* \tag{19}$$

and

$$S_i^* = \sqrt{\frac{1}{n-1}\sum_{j=1}^{n}\left(\bar{X}_{i,j}^* - \bar{\bar{X}}_i^*\right)^2}. \tag{20}$$

It follows that the *i*th sample CV of the measured characteristic $\bar{X}_{i,j}^*$ is

$$\hat{\gamma}_i^* = \frac{S_i^*}{\bar{\bar{X}}_i^*}. \tag{21}$$

The cdf and inverse cdf of $\hat{\gamma}^*$ can be obtained using Equations (5) and (6), respectively, by replacing γ with γ^* in Equation (18).

5. SSMGR CV chart with measurement errors

In the presence of measurement errors, the upper and lower control limits of the SSMGR CV-ME chart are denoted by $\mathrm{UCL}_{\mathrm{ME}}$ and $\mathrm{LCL}_{\mathrm{ME}}$, respectively. Both of these control limits can be computed using Equations (7a) and (7b) but by replacing $\hat{\gamma}$, γ_0 and k with $\hat{\gamma}^*$, γ_0^* and k^*, respectively. Note that the value of the $\mathrm{UCL}_{\mathrm{ME}}$ and $\mathrm{LCL}_{\mathrm{ME}}$ limits' constant k^* is chosen to attain a desired in-control performance for the SSMGR CV-ME chart. The in-control CV of $\bar{X}_{i,j}^*$, i.e. γ_0^*, required in the computation of $\mathrm{UCL}_{\mathrm{ME}}$ and $\mathrm{LCL}_{\mathrm{ME}}$ is calculated using Equation (18) by letting $a = 0$ and $b = 1$. The probability that the sample CV of $\bar{X}_{i,j}^*$ is non-conforming, denoted by P^*, is computed using Equation (8) but by substituting $\hat{\gamma}$, γ, UCL and LCL with $\hat{\gamma}^*$, γ^*, $\mathrm{UCL}_{\mathrm{ME}}$ and $\mathrm{LCL}_{\mathrm{ME}}$, respectively. The out-of-control γ^*, denoted as γ_1^* is computed using Equation (18) when $b \neq 1$, where $1 + a\gamma_0$ in Equation (18) can be replaced with b/τ so that a relation between γ_1^* and τ exists (Tran et al [38]). It should be noted that γ_1^* is used to compute P^* when the process is out-of-control.

The ARL and SDRL values of the SSMGR CV-ME chart are computed using Equations (10) and (11), respectively, by means of the Markov chain approach. Here, the computation of the tpm $\boldsymbol{R}$ is made in a similar way to that of the SSMGR CV chart discussed in Section 3, except that P and α are replaced by P^* and α^*, respectively. Note that α^* is computed using Equation (9) but by replacing $\hat{\gamma}$, P, UCL and LCL with $\hat{\gamma}^*$, P^*, $\mathrm{UCL}_{\mathrm{ME}}$ and $\mathrm{LCL}_{\mathrm{ME}}$, respectively. The SSMGR CV-ME chart is implemented in the same way as that for the SSMGR CV chart (see the three step procedure) discussed in Section 3 but by replacing $\hat{\gamma}$, UCL and LCL with $\hat{\gamma}^*$, $\mathrm{UCL}_{\mathrm{ME}}$ and $\mathrm{LCL}_{\mathrm{ME}}$, respectively.

6. Optimal designs

The optimal designs of the SSMGR CV and SSMGR CV-ME charts involve the computation of the charts' respective optimal parameters to minimize ARL(τ) for $\tau \neq 1$. For the SSMGR CV chart, the step-by-step procedure in computing the chart's optimal design parameters k, C_1 and C_2 is as follows:

Step 1. Specify the values of the desired in-control ARL (say ARL(1) = ω), γ_0, shift size τ for which a quick detection is important and sample size n. Furthermore, initialize $C_1 = 0$, $C_2 = 0$, $\text{ARL}_{\min} = \infty$ and $\text{ARL}_{\text{opt}} = \infty$.

Step 2. Set $C_1 = C_1 + 1$.

Step 3. Set $C_2 = C_2 + 1$.

Step 4. Find the value of k by numerically solving the limits UCL and LCL in Equations (7a) and (7b), respectively, so that ARL(1) = ω.

Step 5. Compute ARL (τ) using Equation (10) using the current values of C_1, C_2 and k.

Step 6. If ARL(τ) < $\text{ARL}_{\min}$, then let $\text{ARL}_{\min}$ = ARL(τ) and return to Step 3. Otherwise, proceed to Step 7.

Step 7. If $\text{ARL}_{\min} < \text{ARL}_{\text{opt}}$, then let $\text{ARL}_{\text{opt}} = \text{ARL}_{\min}$ and return to Step 2, while setting $C_2 = 0$. Otherwise, proceed to Step 8.

Step 8. The minimum value of ARL(τ), based on the values of ω, γ_0, τ and n specified in Step 1 is given by ARL_{opt}, while the corresponding values of C_1, C_2 and k that produce this ARL_{opt} value are the optimal choices of parameters for the SSMGR CV chart.

The above-mentioned step-by-step procedure can also be used to compute the optimal parameter combination (C_1^*, C_2^*, k^*) of the SSMGR CV-ME chart. However, for this case, in addition to the values of ω, γ_0, τ and n specified in Step 1, the values of η, B, m and θ also need to be specified in the same step. Furthermore, in the above eight step procedure, C_1, C_2, k, UCL and LCL are replaced by C_1^*, C_2^*, k^*, UCL_{ME} and LCL_{ME}, respectively.

By adopting the above eight step procedure, optimization programs have been written in MATLAB to compute the optimal parameters of the SSMGR CV and SSMGR CV-ME charts that produce the minimum ARL(τ) value (for $\tau \neq 1$), based on the desired input parameters specified in Step 1. The corresponding SDRL(τ) values are also computed. Table 4 presents the optimal parameter combination (C_1, C_2, k) that minimizes ARL(τ) of the SSMGR CV chart for various choices of n, γ_0 and τ. For example, when $\omega = 370$, $n = 5$, $\gamma_0 = 0.05$ and $\tau = 0.5$ are considered, the optimal parameter combination of the SSMGR CV chart are $(k, C_1, C_2) = (0.0843, 1, 7)$, where these parameters produce the smallest value of ARL(0.25) (= 3.12) (see Table 5) among all parameter combinations (k, C_1, C_2) that give $\omega = 370$. The SDRL(0.25) value of the SSMGR CV chart corresponding to $(k, C_1, C_2) = (0.0843, 1, 7)$ is 4.25 (see Table 5).

Tables 6 – 9 present the optimal combinations of parameters (k^*, C_1^*, C_2^*) for the SSMGR CV-ME chart that minimize ARL(τ), as well as the corresponding ARL(τ) and SDRL(τ) values of the chart, for the specified γ_0, τ, n, η, B, m and θ values. Note that, without loss of generality, b = 1 is considered in this research. For example, when the SSMGR CV-ME chart is optimally designed to minimize ARL(0.5), i.e. for $\tau = 0.5$, the optimal parameter combination (k^*, C_1^*, C_2^*)

= (0.0843, 1, 7) is obtained with the corresponding ARL(0.5) = 3.12 and SDRL(0.5) = 4.25, when $n = 5$, $\gamma_0 = 0.05$, $\eta = 0.1$, $B = 1$, $m = 1$ and $\theta = 0$ (see Table 6).

7. Performance evaluation

There are two objectives of this section. In Section 7.1, the performance of the proposed SSMGR CV chart is compared with those of existing CV charts, while in Section 7.2, the performance of the SSMGR CV-ME chart is investigated in the presence of measurement errors.

7.1 Performance comparison of SSMGR CV and existing CV charts

The performances of the proposed SSMGR CV and existing EWMA CV, RS CV and SSGR CV charts are compared using the ARL(τ) and SDRL(τ) criteria. The 7 regions (7R) RS CV chart is considered as Teoh et al [10] showed that the 7R RS CV chart is more efficient than its 4 regions counterpart. Additionally, the synthetic type CV charts are not considered in the comparison as You et al [7] already showed that the SSGR CV chart outperforms the former.

In Table 5, it is obvious that the SSMGR CV chart outperforms the SSGR CV chart for all (γ_0, τ) combinations as the former has a smaller ARL(τ) value than the latter for the same (γ_0, τ) combination. For example, when $\gamma_0 = 0.1$ and $\tau \in \{0.25, 0.5, 0.75, 1.25, 1.5, 2\}$, ARL($\tau$) $\in$ {1.01, 3.14, 52.57, 8.89, 3.13, 1.53} for the SSMGR CV chart, while that for the SSGR CV chart are {1.01, 4.74, 89.66, 15.22, 4.06, 1.66}, where the ARL(τ) values for the former are all lower than that of the latter. In comparison to the EWMA CV and RS CV charts, the SSMGR CV chart generally performs better for all τ values, except for $\tau = 0.75$. For $\tau = 0.75$, the EWMA CV and RS CV charts provide smaller ARL(τ) values compared to the SSMGR CV chart for all values of

γ_0. For instance, when $\gamma_0 \in \{0.05, 0.1, 0.15, 0.2\}$, the ARL(0.75) values of the EWMA CV and RS CV charts are {17.19, 17.30, 17.49, 17.78} and {22.21, 22.30, 22.45, 22.72}, respectively, while those of the SSMGR CV chart are {51.99, 52.57, 53.50, 54.86}, where it is obvious that the ARL(0.75) values of the SSMGR CV chart are all greater than those of the EWMA CV and RS CV charts. However, for values of $\tau \neq 0.75$, the SSMGR CV chart has smaller ARL(τ) values than those of the EWMA CV and RS CV charts (see Table 5).

In terms of the SDRL(τ) criterion, it is also noticeable in Table 5 that the SSMGR CV chart (lower SDRL(τ) values) significantly prevails over the SSGR CV chart (higher SDRL(τ) values), for all values of τ (except $\tau = 0.75$). In addition, for all γ_0 values based on the SDRL(τ) criterion, the SSMGR CV chart is inferior to the EWMA CV chart when $0.5 \leq \tau \leq 1.25$, while the RS CV chart prevails over the SSMGR CV chart when $0.5 \leq \tau \leq 0.75$. For example, when $\gamma_0 = 0.1$ and $\tau = 0.5$, SDRL(0.5) of the EWMA CV, RS CV and SSMGR CV charts are 1.55, 1.51 and 4.30, respectively, where the values of SDRL(τ) for the EWMA CV and RS CV charts are lower than those of the SSMGR CV chart. For the other values of τ not discussed above, the SSMGR CV chart outperforms the EWMA CV and RS CV charts based on the SDRL(τ) criterion. For instance, when $\gamma_0 = 0.05$ and $\tau = 0.25$, SDRL(0.25) = 0.39, 0.99 and 0.10 for the EWMA CV, RS CV and SSMGR CV charts, respectively, where the SSMGR CV chart has the smallest SDRL(0.25) value.

7.2. Performance of the SSMGR CV-ME chart in the presence of measurement errors

Tables 6 – 9 present the optimal combinations of parameters $\left(k^*, C_1^*, C_2^*\right)$, as well as the corresponding minimum ARL(τ) values and SDRL(τ) values of the SSMGR CV-ME chart based

on the linear covariate error model, for fixed γ_0, τ, n, η, B, m and θ values that satisfy ARL(1) = 370.

Table 6 shows the ARL(τ) and SDRL(τ) values of the SSMGR CV-ME chart for various combinations of the precision error ratios $\eta \in \{0, 0.1, 0.3, 0.5, 1\}$, $\gamma_0 \in \{0.05, 0.1, 0.15, 0.2\}$ and $\tau \in \{0.25, 0.5, 0.75, 1.25, 1.5, 2\}$ when $n = 5$, $m = 1$, $B = 1$ and $\theta = 0$. Note that $\eta = 0$ represents the case without measurement error. Additionally, note that when $\eta = \theta = 0$ and $m = B = 1$, the SSMGR CV-ME chart becomes the basic SSMGR CV chart (as in the case of Table 6). Thus, when $\eta = 0$ in Table 6, the optimal parameters $\left(k^*, C_1^*, C_2^*\right)$ that minimize ARL(τ) of the SSMGR CV-ME chart are not given as they are actually similar to the optimal parameters $\left(k, C_1, C_2\right)$ of the SSMGR CV chart (without measurement error) in Table 4. It is obvious from Table 6 that the precision error ratio (η) has a negative effect on the performance of the SSMGR CV-ME chart as, generally, there are slight increases in the ARL(τ) and SDRL(τ) values when η increases. For example, when $\gamma_0 = 0.1$ and $\tau = 0.75$, ARL(0.75) $\in \{52.57, 52.76, 53.31\}$ and SDRL(0.75) $\in \{212.90, 213.80, 217.40\}$ for $\eta \in \{0, 0.5, 1\}$, where it is found that both ARL(0.75) and SDRL(0.75) increase slightly with η (see Table 6). However, the results in Table 6 show that the precision error ratio (η) does not have a significant effect on the performance of the SSMGR CV-ME chart.

Table 7 presents the ARL(τ) and SDRL(τ) performances of the SSMGR CV-ME chart for various combinations of $B \in \{1, 2, 3, 4\}$, $\gamma_0 \in \{0.05, 0.1, 0.15, 0.2\}$ and $\tau \in \{0.25, 0.5, 0.75, 1.25, 1.5, 2\}$ when $n = 5$, $\eta = 0.28$, $m = 1$ and $\theta = 0.01$. The rationale for choosing $\eta = 0.28$ is due to the assumption of an acceptable value for the signal-to-noise ratio as explained in Tran at al. [33] In

Table 7, it is noticeable that for the fixed values of n, γ_0, τ, η, m and θ, the value of B has some positive effects on the performance of the SSMGR CV-ME chart as, generally, the ARL(τ) and SDRL(τ) values decrease slightly when B increases. As an example, when $\gamma_0 = 0.15$, $\tau = 0.75$, ARL(0.75) = 55.14 and SDRL(0.75) = 225.91 for $B = 1$, while ARL(0.75) = 53.88 and SDRL(0.75) = 220.08 for $B = 4$ (see Table 7), i.e. both ARL(0.75) and SDRL(0.75) decrease when B increases from 1 to 5.

Linna and Woodall [27] noted that it is better to take multiple measurements per item in each sample to reduce the effect of measurement errors. Table 8 presents the ARL(τ) and SDRL(τ) values of the SSMGR CV-ME chart for various combinations of $m \in \{1, 3, 5, 7\}$, $\gamma_0 \in \{0.05, 0.1, 0.15, 0.2\}$ and $\tau \in \{0.25, 0.5, 0.75, 1.25, 1.5, 2\}$ when $n = 5$, $\eta = 0.28$, $B = 1$ and $\theta = 0.01$. Table 8 shows that increasing the number of measurements per item (m) gives some positive effect on the SSMGR CV-ME chart by slightly reducing the ARL(τ) and SDRL(τ) values of the chart when γ_0, τ, n, η, B and θ are fixed, though the reduction is not large. For example, when $\gamma_0 = 0.2$ and $\tau = 0.75$, ARL(0.75) = 56.62 and SDRL(0.75) = 232.77 for $m = 1$, while ARL(0.75) = 56.41 and SDRL(0.75) = 231.80 for $m = 7$ (see Table 8). It is obvious that the values of ARL(0.75) and SDRL(0.75) reduce when m increases from 1 to 7.

Table 9 shows that the ARL(τ) and SDRL(τ) values of the SSMGR CV-ME chart are slightly negatively influenced by the accuracy error (θ) when γ_0, τ, n (=5), η (=0.28), B (= 1) and m (= 1) are fixed. For instance, when $\gamma_0 = 0.2$ and $\tau = 1.25$, ARL(1.25) = 9.31 and SDRL(1.25) = 17.70 for $\theta = 0$, while ARL(1.25) = 10.24 and SDRL(1.25) = 20.30 for $\theta = 0.05$ (see Table 9), where the values of ARL(1.25) and SDRL(1.25) increase with θ.

8. Implementations

To illustrate the implementation of the SSMGR CV and SSMGR CV-ME charts, real life data from a Tunisian company that manufactures sanitary parts from zinc alloy in a die casting hot chamber process are adopted from Castagliola et al [4] The quality characteristic of interest *X* is the weight (in grams) of scrap zinc alloy material (see Castagliola et al [4] for details of the process). Table 10 gives the Phase-I and Phase-II datasets of this quality characteristic. A regression study was conducted by Castagliola et al [4] on the 30 Phase-I samples, each having 5 observations, where a constant proportionality ($\sigma = \gamma \times \mu$) between the process standard deviation σ and the process mean μ of the weight of scrap zinc alloy was found to exist. Castagliola et al [4] also showed that the Phase-I data are in-control. By adopting the root mean square method on the Phase-I samples, the estimated in-control CV $(\hat{\gamma}_0)$ is computed as

$$\hat{\gamma}_0 = \sqrt{\frac{1}{30}\sum_{i=1}^{30}\hat{\gamma}_i^2} = 0.0108,$$

which can be rounded to $\hat{\gamma}_0 = 0.01$.

Suppose that a process engineer has decided to implement the SSMGR CV and SSMGR CV-ME charts for monitoring the Phase-II process. It is assumed that the SSMGR CV chart is optimally designed, based on ARL(1) = 370, $n = 5$ and $\gamma_0 = 0.01$ (as $\hat{\gamma}_0 \approx 0.01$); while the SSMGR CV-ME chart is optimally designed based on ARL(1) = 370, $n = 5$, $\gamma_0 = 0.01$, $\eta = 0.28$, $B = 1$, $m = 1$ and $\theta = 0$. An upward shift in the process CV, where a quick detection is important is set as $\tau = 1.5$, for both the charts. Consequently, the optimal parameters $k = 0.0701$, $C_1 = 1$ and $C_2 = 11$ are computed using the Matlab optimization program for the SSMGR CV chart, where the limits of the chart are computed to be UCL = 0.0161 and LCL = 0.0038. Similarly, the optimal parameters

of the SSMGR CV-ME chart, i.e. $k^* = 0.0701$, $C_1^* = 1$ and $C_2^* = 11$, are computed, which result in $\text{UCL}_{\text{ME}} = 0.0167$ and $\text{LCL}_{\text{ME}} = 0.0040$.

From the control limits of the two charts given in the previous paragraph, it is found that the SSMGR CV chart has tighter limits (narrower width between UCL and LCL, where UCL – LCL = 0.0123) than the SSMGR CV-ME chart (wider width between UCL_{ME} and LCL_{ME}, where $\text{UCL}_{\text{ME}} - \text{LCL}_{\text{ME}} = 0.0127$). Therefore, in general, it becomes easier for the SSMGR CV chart to issue an out-of-control signal, either due to the occurrence of an assignable cause or the presence of measurement errors or both, as the chart's limits have become tighter. However, for the SSMGR CV-ME chart, as its limits have become looser (compared to the SSMGR CV chart), it is in general more difficult to detect an out-of-control signal (compared to the SSMGR CV chart). Hence, when the SSMGR CV-ME chart detects an out-of-control signal, the signal is more likely due to actual process shifts, instead of measurement errors, as its limits have been computed by considering the presence of measurement errors.

The 30 Phase-II sample CVs ($\hat{\gamma}_i$, for $i = 1, 2, \ldots, 30$) are plotted in Figure 1. From Figure 1, it is obvious that the 1st non-conforming $\hat{\gamma}_i$ occurs at sample no., $i = 9$, for both the SSMGR CV and SSMGR CV-ME charts. Thus, $\text{CRL}_1 = 9$ is obtained. The 2nd, 3rd and 4th non-conforming samples are observed at sample nos., $i = 10$, 12 and 13, hence, $\text{CRL}_2 = 1$, $\text{CRL}_3 = 2$ and $\text{CRL}_4 = 1$ are computed for both the charts. Since CRL_1 (= 9) $\leq C_2 = C_2^*$ (= 11), then according to Step 3 of the implementation procedure in Section 3, the SSMGR CV and SSMGR CV-ME charts issue the first out-of-control signal at sample 9 ($i = 9$) (see Figure 1). Following this out-of-control signal, corrective actions should be taken so that the out-of-control process returns to the in-control situation again.

9. Conclusions

There are many circumstances where the mean and standard deviation of a manufacturing process vary in a proportional manner. The CV is a suitable quality characteristic for monitoring the process stability of this type of process. In this research, we have introduced a new CV chart, called the SSMGR CV chart, for efficiently monitoring the CV. The SSMGR CV chart has been compared with the existing EWMA CV, RS CV and SSGR CV charts using the ARL and SDRL as performance criteria. The ARL results have shown that the SSMGR CV chart outperforms the three aforementioned existing CV charts in detecting increasing CV shifts ($\tau > 1$); while for detecting decreasing CV shifts ($\tau < 1$), the SSMGR CV-ME chart still prevails, except for $\tau = 0.75$, where the EWMA CV and RS CV charts beat the former. Based on the findings in this research, we recommend the use of the SSMGR CV chart when the process engineer is interested to monitor upward shifts ($\tau > 1$) or moderate-to-large downward shifts ($\tau < 1$), in the process CV.

When a process being monitored is in-control, ideally the ratio of the standard deviation to the mean, i.e. $\gamma_0 = \sigma_0/\mu_0$ should be small so that the process is operating reliably. Note that the data employed to illustrate the implementations of the CV charts in practice by Kang et al, [1] Khaw et al, [11] and Yeong et al, [42] all deal with small γ_0 values, namely 0.075, 0.005645 and 0.001042, respectively. Thus, small γ_0 values, i.e. $\gamma_0 \in \{0.05, 0.1, 0.15, 0.2\}$ are adopted in this article.

This research has also investigated the effect of measurement errors on the SSMGR CV (referred to as the SSMGR CV-ME) chart. The findings has revealed that the increases in the precision error ratio (η) or accuracy error (θ) has a negative effect on the SSMGR CV-ME chart's performance by slightly increasing its ARL(τ) and SDRL(τ) values for a similar shift size τ. Furthermore, increasing the number of measurements per item (m) or the parameter B has a

positive effect on the ARL(τ) and SDRL(τ) performances of the SSMGR CV-ME chart as their values decrease slightly when m or B increases.

In this research, the univariate SSMGR CV and SSMGR CV-ME charts have been developed to monitor the process CV. In the future, research may be conducted to develop the multivariate SSMGR CV and SSMGR CV-ME charts. Moreover, univariate and multivariate SSMGR CV and SSMGR CV-ME charts with estimated process parameters, i.e. when the target values of the process parameters are unknown or cannot be specified, can also be proposed.

Acknowledgments

This work is supported by the Miyan Research Institute, International University of Business Agriculture and Technology, Dhaka, Bangladesh.

References

1. Kang C, Lee M, Seong Y, Hawkins D. A control chart for the coefficient of variation. *Journal of Quality Technology* 2007; **39**: 151-158.
2. Hong EP, Kang CW, Baek JW, Kang HW. Development of CV control chart using EWMA technique. *Journal of the Society of Korea Industrial and Systems Engineering* 2008; **31**: 114-120.
3. Castagliola P, Celano G, Psarakis S. Monitoring the coefficient of variation using EWMA charts. *Journal of Quality Technology* 2011; **43**: 249-265.
4. Castagliola P, Achouri A, Taleb, H, Celano G, Psarakis S. Monitoring the coefficient of variation using a variable sampling interval control chart. *Quality and Reliability Engineering International* 2013; **29**: 1135-1149.

5. Castagliola P, Achouri A, Taleb H, Celano G, Psarakis S. Monitoring the coefficient of variation using a variable sample size control chart. *The International Journal of Advanced Manufacturing Technology* 2015; **80**: 1561-1576.
6. Calzada ME, Scariano SM. A synthetic control chart for the coefficient of variation. *Journal of Statistical Computation and Simulation* 2013; **83**: 853-867.
7. You HW, Khoo MBC, Castagliola P, Haq A. Monitoring the coefficient of variation using the side sensitive group runs chart. *Quality and Reliability Engineering International* 2016; **32**: 1913-1927.
8. Noor-ul-Amin M, Tariq S, Hanif M. Control charts for simultaneously monitoring of process mean and coefficient of variation with and without auxiliary information. *Quality and Reliability Engineering International* 2019; **35:** 2639-2656.
9. Giner-Bosch V, Tran KP, Castagliola P, Khoo MBC. An EWMA control chart for the multivariate coefficient of variation. *Quality and Reliability Engineering International* 2019; **35:** 1515-1541.
10. Teoh WL, Khoo MBC, Castagliola P, Yeong WC, Teh SY. Run-sum control charts for monitoring the coefficient of variation. *European Journal of Operational Research* 2017; **257**: 144-158.
11. Khaw KW, Khoo MBC, Yeong WC, Wu Z. Monitoring the coefficient of variation using a variable sample size and sampling interval control chart. *Communications in Statistics-Simulation and Computation* 2017; **46**: 5772-5794.
12. Yeong WC, Khoo MBC, Lim SL, Teoh WL. The coefficient of variation chart with measurement error. *Quality Technology & Quantitative Management* 2017; **14**: 353-377.

13. Yeong WC, Lim SL, Khoo MBC, Castagliola P. Monitoring the coefficient of variation using a variable parameters chart. *Quality Engineering* 2018; **30**: 212-235.
14. Chew XY, Khoo MBC, Khaw KW, Yeong WC, Chong ZL. A proposed variable parameter control chart for monitoring the multivariate coefficient of variation. *Quality and Reliability Engineering International* 2019; **35**: 2442-2461.
15. Wu Z, Spedding TA. A synthetic control chart for detecting small shifts in the process mean. *Journal of Quality Technology* 2000; **32**: 32-38.
16. Gadre MP, Rattihalli RN. A group runs control chart for detecting shifts in the process mean. *Economic Quality Control* 2004; **19**: 29-43.
17. Gadre MP, Rattihalli RN. Modified group runs control charts to detect increases in fraction nonconforming and shifts in the process mean. *Communications in Statistics - Simulation and Computation* 2006; **35**: 225-240.
18. Gadre MP, Rattihalli RN. A side sensitive group runs control chart for detecting shifts in the process mean. *Statistical Methods and Applications* 2007; **16**: 27-37.
19. Gadre MP, Joshi KA, Rattihalli RN. A side sensitive modified group runs control chart to detect shifts in the process mean. *Journal of Applied Statistics* 2010; **37**: 2073-2087.
20. You HW, Khoo MBC, Castagliola P, Ou Y. Side sensitive group runs $\bar{X}$ chart with estimated process parameters. *Computational Statistics* 2015; **30**: 1245-1278.
21. Khoo MBC, Tan EK, Chong ZL, Haridy S. Side-sensitive group runs double sampling (SSGRDS) chart for detecting mean shifts. *International Journal of Production Research* 2015; **53**: 4735-4753.
22. Chong ZL, Khoo MBC, Lee MH, Chen CH. Group runs revised m-of-k runs rule control chart. *Communications in Statistics - Theory and Methods* 2017; **46**: 6916-6935.

23. Saha S, Khoo MBC, Lee MH, Castagliola P. A side-sensitive modified group runs double sampling (SSMGRDS) control chart for detecting mean shifts. *Communications in Statistics - Simulation and Computation* 2018; **47**: 1353-1369.

24. Chong ZL, Khoo MBC, Teoh WL, You HW, Castagliola P. Optimal design of the side-sensitive modified group runs (SSMGR) chart when process parameters are estimated. *Quality and Reliability Engineering International* 2019; **35**: 246-262.

25. Mim FN, Saha S, Khoo MBC, Khatun M. A Side-sensitive modified group runs control chart with auxiliary information to detect process mean shifts. *Pertanika Journal of Science & Technology* 2019; **27**: 847 – 866.

26. Gadre MP, Kakade VC. Some side sensitive group runs based control charts to detect shifts in the process median. *Communications in Statistics - Simulation and Computation* 2019; doi.org/10.1080/03610918.2019.1672736.

27. Linna KW, Woodall WH. Effect of measurement error on Shewhart control charts. *Journal of Quality Technology* 2001; **33**: 213-222.

28. Linna KW, Woodall WH, Busby KL. The performance of multivariate control charts in the presence of measurement error. *Journal of Quality Technology* 2001; **33**; 349-355.

29. Costa AFB, Castagliola P. Effect of measurement error and autocorrelation on the $\bar{X}$ chart. *Journal of Applied Statistics* 2011; **38**: 661-673.

30. Nguyen HD, Tran KP. Effect of the measurement errors on two one-sided Shewhart control charts for monitoring the ratio of two normal variables. *Quality and Reliability Engineering International* **2020**: doi.org/10.1002/qre.2656.

31. Tran PH, Tran KP, Rakitzis A. A Synthetic median control chart for monitoring the process mean with measurement errors. *Quality and Reliability Engineering International* 2019; **35**: 1100-1116.
32. Maravelakis PE. Measurement error effect on the CUSUM control chart. *Journal of Applied Statistics* 2012; **39**: 323-336.
33. Hu X, Castagliola P, Sun J, Khoo MBC. The effect of measurement errors on the synthetic chart. *Quality and Reliability Engineering International* 2015; **31**: 1769-1778.
34. Noorossana R, Zerehsaz Y. Effect of measurement error on phase II monitoring of simple linear profiles. *The International Journal of Advanced Manufacturing Technology* 2015; **79**: 2031-2040.
35. Tran KP, Castagliola P, Celano G. The performance of the Shewhart-RZ control chart in the presence of measurement error. *International Journal of Production Research* 2016; **54**: 7504-7522.
36. Tran KP, Castagliola P, Balakrishnan N. On the performance of Shewhart median chart in the presence of measurement errors. *Quality and Reliability Engineering International* 2017; **33**: 1019-1029.
37. Yeong WC, Khoo MBC, Tham LK, Teoh WL, Rahim MA. Monitoring the coefficient of variation using a variable sampling interval EWMA chart. *Journal of Quality Technology* 2017; **49**: 380-401.
38. Tran KP, Heuchenne C, Balakrishnan N. On the performance of coefficient of variation charts in the presence of measurement errors. *Quality and Reliability Engineering International* 2019; **35**: 329-350.

39. McKay AT. Distribution of the Coefficient of Variation and the Extended "*t*" Distribution. *Journal of the Royal Statistical Society* 1932; **95**: 695-698.
40. Iglewicz B, Myers RH, Howe RB. On the percentage points of the sample coefficient of variation. *Biometrika* 1968; **55**: 580-581.
41. Iglewicz B, Myers RH. Comparisons of Approximations to the Percentage Points of the Sample Coefficient of Variation. *Technometrics* 1970; **12**: 166-169.
42. Yeong WC, Khoo MBC, Teoh WL, Castagliola P. A control chart for the multivariate coefficient of variation. *Quality and Reliability Engineering International* 2016; **32:** 1213-1225.

Table 1. Descriptions of the Markov chain states of the samples for the SSMGR CV chart

State	Description	State	Description
$\underline{\bar{G}}$	The sample at time zero is non-conforming and the corresponding CRL does not exceed C_1, where there is either an upward or a downward process mean shift.	$\bar{G}(\bar{H})$	A sequence showing the non-absorbing state, ending with the sample in the first (second) level of sample inspection being non-conforming with an upward process mean shift.
G	The non-conforming sample in the first level of sample inspection has a process mean shift on any side with CRL > C_1.	$\underline{G}(\underline{H})$	A sequence showing the non-absorbing state, ending with the sample in the first (second) level of sample inspection being non-conforming with a downward process mean shift.
$0\,(\tilde{0})$	The sample in the first (second) level of sample inspection is conforming.		

Table 2. The Markov chain states of the SSMGR CV chart for $C_1 = C_2 = 3$

State no.	State	State no.	State	State no.	State
1	$\underline{\bar{G}}$	8	$\bar{G}\,\tilde{0}$	15	$\bar{H}$
2	$\underline{\bar{G}}\,\tilde{0}$	9	$\bar{G}\,\tilde{0}\tilde{0}$	16	$\bar{H}\,0$
3	$\underline{\bar{G}}\,\tilde{0}\tilde{0}$	10	$\underline{G}\,\tilde{0}$	17	$\bar{H}\,00$
4	$\tilde{0}\tilde{0}\tilde{0}$	11	$\underline{G}\,\tilde{0}\tilde{0}$	18	$\underline{H}$
5	$\bar{G}$	12	G	19	$\underline{H}0$
6	$\underline{G}$	13	$G0$	20	$\underline{H}00$
7	000	14	$G00$	21	Signal

Table 3. The tpm of the Markov chain model of the SSMGR CV chart for $C_1 = C_2 = 3$

State	State h																			
g	1	2	3	4	5	6	7	8	9	10	11	12	13	14	15	16	17	18	19	20
1	0	T	0	0	0	0	0	0	0	0	0	0	0	0	0	0	0	0	0	0
2	0	0	T	0	0	0	0	0	0	0	0	0	0	0	0	0	0	0	0	0
3	0	0	0	T	0	0	0	0	0	0	0	0	0	0	0	0	0	0	0	0
4	0	0	0	T	0	0	0	0	0	0	0	S	0	0	0	0	0	0	0	0
5	0	0	0	0	0	0	0	T	0	0	0	0	0	0	0	0	0	$(1-\alpha)S$	0	0
6	0	0	0	0	0	0	0	0	0	T	0	0	0	0	αS	0	0	0	0	0
7	0	0	0	0	0	0	T	0	0	0	0	S	0	0	0	0	0	0	0	0
8	0	0	0	0	0	0	0	0	T	0	0	0	0	0	0	0	0	$(1-\alpha)S$	0	0
9	0	0	0	T	0	0	0	0	0	0	0	0	0	0	0	0	0	$(1-\alpha)S$	0	0
10	0	0	0	0	0	0	0	0	0	0	T	0	0	0	αS	0	0	0	0	0
11	0	0	0	T	0	0	0	0	0	0	0	0	0	0	αS	0	0	0	0	0
12	0	0	0	0	αS	$(1-\alpha)S$	0	0	0	0	0	0	T	0	0	0	0	0	0	0
13	0	0	0	0	αS	$(1-\alpha)S$	0	0	0	0	0	0	0	T	0	0	0	0	0	0
14	0	0	0	0	αS	$(1-\alpha)S$	T	0	0	0	0	0	0	0	0	0	0	0	0	0
15	0	0	0	0	αS	$(1-\alpha)S$	0	0	0	0	0	0	0	0	0	T	0	0	0	0
16	0	0	0	0	αS	$(1-\alpha)S$	0	0	0	0	0	0	0	0	0	0	T	0	0	0
17	0	0	0	0	αS	$(1-\alpha)S$	T	0	0	0	0	0	0	0	0	0	0	0	0	0
18	0	0	0	0	αS	$(1-\alpha)S$	0	0	0	0	0	0	0	0	0	0	0	0	T	0
19	0	0	0	0	αS	$(1-\alpha)S$	0	0	0	0	0	0	0	0	0	0	0	0	0	T
20	0	0	0	0	αS	$(1-\alpha)S$	T	0	0	0	0	0	0	0	0	0	0	0	0	0

Table 4. Optimal parameters of the SSMGR CV chart when $\omega = 370$

		$n = 5$			$n = 7$			$n = 10$		
γ_0	τ	k	C_1	C_2	k	C_1	C_2	k	C_1	C_2
0.05	0.25	0.1359	1	2	0.1359	1	2	0.1359	1	2
	0.5	0.0843	1	7	0.1169	1	3	0.1359	1	2
	0.75	0.0254	1	92	0.0365	1	46	0.0530	1	21
	1.25	0.0430	1	33	0.0499	1	24	0.0582	1	17
	1.5	0.0701	1	11	0.0799	1	8	0.0896	1	6
	2	0.0962	1	5	0.1049	1	4	0.1169	1	3
0.1	0.25	0.1359	1	2	0.1359	1	2	0.1359	1	2
	0.5	0.0843	1	7	0.1169	1	3	0.1359	1	2
	0.75	0.0254	1	92	0.0361	1	47	0.0530	1	21
	1.25	0.0430	1	33	0.0499	1	24	0.0582	1	17
	1.5	0.0701	1	11	0.0799	1	8	0.0896	1	6
	2	0.0962	1	5	0.1049	1	4	0.1169	1	3
0.15	0.25	0.1359	1	2	0.1359	1	2	0.1359	1	2
	0.5	0.0843	1	7	0.1049	1	4	0.1359	1	2
	0.75	0.0251	1	94	0.0357	1	48	0.0519	1	22
	1.25	0.0424	1	34	0.0489	1	25	0.0582	1	17
	1.5	0.0701	1	11	0.0799	1	8	0.0896	1	6
	2	0.0962	1	5	0.1049	1	4	0.1169	1	3
0.2	0.25	0.1359	1	2	0.1359	1	2	0.1359	1	2
	0.5	0.0843	1	7	0.1049	1	4	0.1359	1	2
	0.75	0.0251	1	94	0.0350	1	50	0.0508	1	23
	1.25	0.0418	1	35	0.0489	1	25	0.0567	1	18
	1.5	0.0701	1	11	0.0799	1	8	0.0896	1	6
	2	0.0962	1	5	0.1049	1	4	0.1169	1	3

Table 5. ARL(τ) and SDRL(τ) values of the EWMA CV, RS CV, SSGR CV and SSMGR CV charts when $\omega = 370$ and $n = 5$

		EWMA CV		RS CV		SSGR CV		SSMGR CV	
γ_0	τ	ARL(τ)	SDRL(τ)	ARL(τ)	SDRL(τ)	ARL(τ)	SDRL(τ)	ARL(τ)	SDRL(τ)
0.05	0.25	3.10	0.39	2.72	0.99	1.01	0.19	1.01	0.10
	0.5	5.92	1.54	5.42	1.50	4.70	6.62	3.12	4.25
	0.75	17.19	7.03	22.21	17.12	88.90	122.69	51.99	210.20
	1.25	15.58	11.38	18.92	16.96	15.02	22.02	8.79	16.22
	1.5	5.64	4.00	5.94	4.53	4.00	4.68	3.09	3.42
	2	2.32	1.51	2.34	1.51	1.64	1.28	1.52	1.00
0.1	0.25	3.13	0.38	2.78	1.04	1.01	0.19	1.01	0.10
	0.5	5.99	1.55	5.44	1.51	4.74	6.69	3.14	4.30
	0.75	17.30	7.04	22.30	17.19	89.66	123.67	52.57	212.90
	1.25	15.64	11.44	19.09	17.16	15.22	22.37	8.89	16.60
	1.5	5.69	4.02	6.01	4.60	4.06	4.78	3.13	3.50
	2	2.35	1.53	2.38	1.54	1.66	1.32	1.53	1.03
0.15	0.25	3.19	0.41	2.89	1.13	1.01	0.20	1.01	0.10
	0.5	6.09	1.54	5.46	1.53	4.81	6.80	3.18	4.39
	0.75	17.49	7.17	22.45	17.33	90.93	125.31	53.50	218.31
	1.25	15.75	11.55	19.41	17.42	15.56	22.96	9.05	16.92
	1.5	5.77	4.06	6.14	4.71	4.15	4.95	3.18	3.64
	2	2.41	1.57	2.44	1.60	1.70	1.38	1.56	1.08
0.2	0.25	3.28	0.46	3.02	0.99	1.01	0.20	1.01	0.11
	0.5	6.25	1.54	5.49	1.55	4.91	6.96	3.23	4.52
	0.75	17.78	7.29	22.72	17.57	92.69	127.58	54.86	224.65
	1.25	15.90	11.70	19.87	17.93	16.04	23.51	9.27	17.53
	1.5	5.88	4.13	6.31	4.86	4.29	5.20	3.27	3.86
	2	2.49	1.62	2.52	1.68	1.75	1.47	1.59	1.14

Table 6. ARL(τ) and SDRL(τ) values of the SSMGR CV-ME chart in the presence of measurement errors for various values of τ, γ_0 and η when $n = 5$, $m = 1$, $B = 1$ and $\theta = 0$

		$\eta = 0$		$\eta = 0.1$					$\eta = 0.3$					$\eta = 0.5$					$\eta = 1$				
γ_0	τ	ARL(τ)	SDRL(τ)	k^*	C_1^*	C_2^*	ARL(τ)	SDRL(τ)	k^*	C_1^*	C_2^*	ARL(τ)	SDRL(τ)	k^*	C_1^*	C_2^*	ARL(τ)	SDRL(τ)	k^*	C_1^*	C_2^*	ARL(τ)	SDRL(τ)
0.05	0.25	1.01	0.10	0.1359	1	2	1.01	0.10	0.1359	1	2	1.01	0.10	0.1359	1	2	1.01	0.10	0.1359	1	2	1.01	0.10
	0.5	3.12	4.25	0.0843	1	7	3.12	4.25	0.0843	1	7	3.12	4.25	0.0843	1	7	3.12	4.26	0.0843	1	7	3.13	4.27
	0.75	51.99	210.20	0.0254	1	92	51.99	210.21	0.0254	1	92	52.00	210.29	0.0254	1	92	52.03	210.43	0.0254	1	92	52.18	211.10
	1.25	8.79	16.22	0.0430	1	33	8.80	16.22	0.0430	1	33	8.80	16.23	0.0430	1	33	8.80	16.25	0.0430	1	33	8.83	16.35
	1.5	3.09	3.42	0.0701	1	11	3.09	3.42	0.0701	1	11	3.09	3.42	0.0701	1	11	3.09	3.42	0.0701	1	11	3.10	3.44
	2	1.52	1.00	0.0962	1	5	1.52	1.00	0.0962	1	5	1.52	1.00	0.0962	1	5	1.52	1.01	0.0962	1	5	1.52	1.01
0.1	0.25	1.01	0.10	0.1359	1	2	1.01	0.10	0.1359	1	2	1.01	0.10	0.1359	1	2	1.01	0.10	0.1359	1	2	1.01	0.10
	0.5	3.14	4.30	0.0843	1	7	3.14	4.31	0.0843	1	7	3.14	4.31	0.0843	1	7	3.15	4.32	0.0843	1	7	3.17	4.38
	0.75	52.57	212.90	0.0254	1	92	52.57	212.93	0.0254	1	92	52.64	213.22	0.0254	1	92	52.76	213.80	0.0251	1	94	53.31	217.40
	1.25	8.89	16.60	0.0430	1	33	8.89	16.61	0.0430	1	33	8.90	16.65	0.0424	1	34	8.92	16.70	0.0424	1	34	9.01	16.79
	1.5	3.13	3.50	0.0701	1	11	3.13	3.50	0.0701	1	11	3.13	3.51	0.0701	1	11	3.14	3.53	0.0701	1	11	3.17	3.61
	2	1.53	1.03	0.0962	1	5	1.53	1.03	0.0962	1	5	1.54	1.03	0.0962	1	5	1.54	1.04	0.0962	1	5	1.55	1.07
0.15	0.25	1.01	0.10	0.1359	1	2	1.01	0.10	0.1359	1	2	1.01	0.10	0.1359	1	2	1.01	0.11	0.1359	1	2	1.01	0.11
	0.5	3.18	4.39	0.0843	1	7	3.18	4.40	0.0843	1	7	3.18	4.41	0.0843	1	7	3.19	4.44	0.0843	1	7	3.24	4.56
	0.75	53.50	218.31	0.0251	1	94	53.52	218.39	0.0251	1	94	53.66	219.04	0.0251	1	94	53.94	220.35	0.0251	1	94	55.25	226.46
	1.25	9.05	16.92	0.0424	1	34	9.05	16.93	0.0424	1	34	9.07	17.03	0.0424	1	34	9.12	17.22	0.0418	1	35	9.34	17.81
	1.5	3.18	3.64	0.0701	1	11	3.18	3.65	0.0701	1	11	3.19	3.67	0.0701	1	11	3.21	3.71	0.0676	1	12	3.29	3.71
	2	1.56	1.08	0.0962	1	5	1.56	1.08	0.0962	1	5	1.56	1.08	0.0962	1	5	1.57	1.10	0.0962	1	5	1.61	1.16
0.2	0.25	1.01	0.11	0.1359	1	2	1.01	0.11	0.1359	1	2	1.01	0.11	0.1359	1	2	1.01	0.11	0.1359	1	2	1.01	0.12
	0.5	3.23	4.52	0.0843	1	7	3.23	4.53	0.0843	1	7	3.24	4.55	0.0843	1	7	3.26	4.60	0.0843	1	7	3.35	4.82
	0.75	54.86	224.65	0.0251	1	94	54.89	224.79	0.0251	1	94	55.14	225.95	0.0251	1	94	55.64	228.27	0.0251	1	94	58.01	239.14
	1.25	9.27	17.53	0.0418	1	35	9.28	17.55	0.0418	1	35	9.32	17.73	0.0418	1	35	9.41	18.10	0.0407	1	37	9.83	19.19
	1.5	3.27	3.86	0.0701	1	11	3.27	3.86	0.0676	1	12	3.29	3.70	0.0676	1	12	3.32	3.77	0.0676	1	12	3.47	4.15
	2	1.59	1.14	0.0962	1	5	1.60	1.14	0.0962	1	5	1.60	1.16	0.0962	1	5	1.62	1.18	0.0962	1	5	1.68	1.31

Table 7. ARL(τ) and SDRL(τ) values of the SSMGR CV-ME chart in the presence of measurement errors for various values of τ, γ_0 and B when $n = 5$, $\eta = 0.28$, $m = 1$ and $\theta = 0.01$

		$B = 1$					$B = 2$					$B = 3$					$B = 4$				
γ_0	τ	k^*	C_1^*	C_2^*	ARL(τ)	SDRL(τ)	k^*	C_1^*	C_2^*	ARL(τ)	SDRL(τ)	k^*	C_1^*	C_2^*	ARL(τ)	SDRL(τ)	k^*	C_1^*	C_2^*	ARL(τ)	SDRL(τ)
0.05	0.25	0.1359	1	2	1.01	0.11	0.1359	1	2	1.01	0.10	0.1359	1	2	1.01	0.10	0.1359	1	2	1.01	0.10
	0.5	0.0843	1	7	3.18	4.41	0.0843	1	7	3.15	4.33	0.0843	1	7	3.14	4.30	0.0843	1	7	3.13	4.29
	0.75	0.0251	1	94	53.45	218.08	0.0254	1	92	52.73	213.65	0.0254	1	92	52.48	212.50	0.0254	1	92	52.36	211.92
	1.25	0.0424	1	34	8.98	16.64	0.0430	1	33	8.89	16.60	0.0430	1	33	8.86	16.47	0.0430	1	33	8.84	16.41
	1.5	0.0701	1	11	3.15	3.57	0.0701	1	11	3.12	3.49	0.0701	1	11	3.11	3.47	0.0701	1	11	3.11	3.45
	2	0.0962	1	5	1.54	1.04	0.0962	1	5	1.53	1.02	0.0962	1	5	1.53	1.02	0.0962	1	5	1.52	1.01
0.1	0.25	0.1359	1	2	1.01	0.11	0.1359	1	2	1.01	0.10	0.1359	1	2	1.01	0.10	0.1359	1	2	1.01	0.10
	0.5	0.0843	1	7	3.21	4.47	0.0843	1	7	3.17	4.39	0.0843	1	7	3.16	4.36	0.0843	1	7	3.16	4.35
	0.75	0.0251	1	94	54.08	221.01	0.0251	1	94	53.29	217.31	0.0254	1	92	53.07	215.22	0.0254	1	92	52.94	214.63
	1.25	0.0424	1	34	9.08	17.06	0.0424	1	34	8.98	16.65	0.0424	1	34	8.95	16.52	0.0424	1	34	8.93	16.46
	1.5	0.0701	1	11	3.19	3.66	0.0701	1	11	3.16	3.58	0.0701	1	11	3.15	3.55	0.0701	1	11	3.14	3.54
	2	0.0962	1	5	1.56	1.07	0.0962	1	5	1.55	1.05	0.0962	1	5	1.54	1.04	0.0962	1	5	1.54	1.04
0.15	0.25	0.1359	1	2	1.01	0.11	0.1359	1	2	1.01	0.11	0.1359	1	2	1.01	0.11	0.1359	1	2	1.01	0.11
	0.5	0.0843	1	7	3.25	4.57	0.0843	1	7	3.21	4.48	0.0843	1	7	3.20	4.45	0.0843	1	7	3.19	4.44
	0.75	0.0251	1	94	55.14	225.91	0.0251	1	94	54.28	221.94	0.0251	1	94	54.01	220.69	0.0251	1	94	53.88	220.08
	1.25	0.0418	1	35	9.25	17.43	0.0418	1	35	9.14	16.98	0.0424	1	34	9.11	17.18	0.0424	1	34	9.09	17.11
	1.5	0.0701	1	11	3.25	3.82	0.0701	1	11	3.22	3.73	0.0701	1	11	3.20	3.70	0.0701	1	11	3.20	3.68
	2	0.0962	1	5	1.58	1.12	0.0962	1	5	1.57	1.10	0.0962	1	5	1.57	1.09	0.0962	1	5	1.56	1.09
0.2	0.25	0.1359	1	2	1.01	0.11	0.1359	1	2	1.01	0.11	0.1359	1	2	1.01	0.11	0.1359	1	2	1.01	0.11
	0.5	0.0843	1	7	3.30	4.71	0.0843	1	7	3.26	4.61	0.0843	1	7	3.25	4.58	0.0843	1	7	3.25	4.57
	0.75	0.0251	1	94	56.62	232.77	0.0251	1	94	55.68	228.42	0.0251	1	94	55.39	227.10	0.0251	1	94	55.25	226.46
	1.25	0.0412	1	36	9.50	18.13	0.0418	1	35	9.37	17.95	0.0418	1	35	9.34	17.80	0.0418	1	35	9.32	17.73
	1.5	0.0676	1	12	3.34	3.84	0.0676	1	12	3.30	3.74	0.0676	1	12	3.29	3.71	0.0676	1	12	3.28	3.69
	2	0.0962	1	5	1.62	1.20	0.0962	1	5	1.61	1.17	0.0962	1	5	1.60	1.16	0.0962	1	5	1.60	1.15

Table 8. ARL(τ) and SDRL(τ) values of the SSMGR CV-ME chart in the presence of measurement errors for various values of τ, γ_0 and m when $n = 5$, $\eta = 0.28$, $B = 1$ and $\theta = 0.01$

		$m = 1$					$m = 3$					$m = 5$					$m = 7$				
γ_0	τ	k^*	C_1^*	C_2^*	ARL(τ)	SDRL(τ)	k^*	C_1^*	C_2^*	ARL(τ)	SDRL(τ)	k^*	C_1^*	C_2^*	ARL(τ)	SDRL(τ)	k^*	C_1^*	C_2^*	ARL(τ)	SDRL(τ)
0.05	0.25	0.1359	1	2	1.01	0.11	0.1359	1	2	1.01	0.11	0.1359	1	2	1.01	0.11	0.1359	1	2	1.01	0.11
	0.5	0.0843	1	7	3.18	4.41	0.0843	1	7	3.18	4.41	0.0843	1	7	3.18	4.41	0.0843	1	7	3.18	4.41
	0.75	0.0251	1	94	53.45	218.08	0.0251	1	94	53.44	218.03	0.0251	1	94	53.44	218.02	0.0251	1	94	53.44	218.01
	1.25	0.0424	1	34	8.98	16.64	0.0424	1	34	8.98	16.64	0.0424	1	34	8.98	16.64	0.0424	1	34	8.98	16.64
	1.5	0.0701	1	11	3.15	3.57	0.0701	1	11	3.15	3.57	0.0701	1	11	3.15	3.57	0.0701	1	11	3.15	3.57
	2	0.0962	1	5	1.54	1.04	0.0962	1	5	1.54	1.04	0.0962	1	5	1.54	1.04	0.0962	1	5	1.54	1.04
0.1	0.25	0.1359	1	2	1.01	0.11	0.1359	1	2	1.01	0.11	0.1359	1	2	1.01	0.11	0.1359	1	2	1.01	0.11
	0.5	0.0843	1	7	3.21	4.47	0.0843	1	7	3.21	4.47	0.0843	1	7	3.21	4.47	0.0843	1	7	3.21	4.47
	0.75	0.0251	1	94	54.08	221.01	0.0251	1	94	54.04	220.82	0.0251	1	94	54.03	220.79	0.0251	1	94	54.03	220.77
	1.25	0.0424	1	34	9.08	17.06	0.0424	1	34	9.07	17.03	0.0424	1	34	9.07	17.03	0.0424	1	34	9.07	17.02
	1.5	0.0701	1	11	3.19	3.66	0.0701	1	11	3.19	3.65	0.0701	1	11	3.19	3.65	0.0701	1	11	3.19	3.65
	2	0.0962	1	5	1.56	1.07	0.0962	1	5	1.56	1.07	0.0962	1	5	1.56	1.07	0.0962	1	5	1.56	1.07
0.15	0.25	0.1359	1	2	1.01	0.11	0.1359	1	2	1.01	0.11	0.1359	1	2	1.01	0.11	0.1359	1	2	1.01	0.11
	0.5	0.0843	1	7	3.25	4.57	0.0843	1	7	3.24	4.56	0.0843	1	7	3.24	4.56	0.0843	1	7	3.24	4.56
	0.75	0.0251	1	94	55.14	225.91	0.0251	1	94	55.04	225.49	0.0251	1	94	55.03	225.40	0.0251	1	94	55.02	225.37
	1.25	0.0418	1	35	9.25	17.43	0.0418	1	35	9.23	17.37	0.0418	1	35	9.23	17.35	0.0418	1	35	9.23	17.35
	1.5	0.0701	1	11	3.25	3.82	0.0701	1	11	3.25	3.80	0.0701	1	11	3.25	3.80	0.0701	1	11	3.25	3.80
	2	0.0962	1	5	1.58	1.12	0.0962	1	5	1.58	1.12	0.0962	1	5	1.58	1.12	0.0962	1	5	1.58	1.12
0.2	0.25	0.1359	1	2	1.01	0.11	0.1359	1	2	1.01	0.11	0.1359	1	2	1.01	0.11	0.1359	1	2	1.01	0.11
	0.5	0.0843	1	7	3.30	4.71	0.0843	1	7	3.30	4.70	0.0843	1	7	3.30	4.69	0.0843	1	7	3.30	4.69
	0.75	0.0251	1	94	56.62	232.77	0.0251	1	94	56.46	232.01	0.0251	1	94	56.42	231.86	0.0251	1	94	56.41	231.80
	1.25	0.0412	1	36	9.50	18.13	0.0412	1	36	9.47	18.01	0.0412	1	36	9.46	17.99	0.0412	1	36	9.46	17.98
	1.5	0.0676	1	12	3.34	3.84	0.0676	1	12	3.33	3.81	0.0676	1	12	3.33	3.81	0.0676	1	12	3.33	3.81
	2	0.0962	1	5	1.62	1.20	0.0962	1	5	1.62	1.19	0.0962	1	5	1.62	1.19	0.0962	1	5	1.62	1.19

Table 9. ARL(τ) and SDRL(τ) values of the SSMGR CV-ME chart in the presence of measurement errors for various values of τ, γ_0 and θ when $n = 5$, $\eta = 0.28$, $B = 1$ and $m = 1$

		$\theta = 0$					$\theta = 0.01$					$\theta = 0.03$					$\theta = 0.05$				
γ_0	τ	k^*	C_1^*	C_2^*	ARL(τ)	SDRL(τ)	k^*	C_1^*	C_2^*	ARL(τ)	SDRL(τ)	k^*	C_1^*	C_2^*	ARL(τ)	SDRL(τ)	k^*	C_1^*	C_2^*	ARL(τ)	SDRL(τ)
0.05	0.25	0.1359	1	2	1.01	0.10	0.1359	1	2	1.01	0.11	0.1359	1	2	1.01	0.12	0.1359	1	2	1.01	0.13
	0.5	0.0843	1	7	3.12	4.25	0.0843	1	7	3.18	4.41	0.0843	1	7	3.32	4.75	0.0799	1	8	3.46	4.91
	0.75	0.0254	1	92	52.00	210.27	0.0251	1	94	53.45	218.08	0.0251	1	94	56.50	232.21	0.0248	1	96	59.63	247.86
	1.25	0.0430	1	33	8.80	16.23	0.0424	1	34	8.98	16.64	0.0418	1	35	9.35	17.85	0.0407	1	37	9.73	18.77
	1.5	0.0701	1	11	3.09	3.42	0.0701	1	11	3.15	3.57	0.0676	1	12	3.28	3.68	0.0676	1	12	3.40	3.99
	2	0.0962	1	5	1.52	1.00	0.0962	1	5	1.54	1.04	0.0962	1	5	1.59	1.13	0.0962	1	5	1.63	1.22
0.1	0.25	0.1359	1	2	1.01	0.10	0.1359	1	2	1.01	0.11	0.1359	1	2	1.01	0.12	0.1359	1	2	1.01	0.13
	0.5	0.0843	1	7	3.14	4.31	0.0843	1	7	3.21	4.47	0.0843	1	7	3.34	4.81	0.0799	1	8	3.48	4.98
	0.75	0.0254	1	92	52.63	213.18	0.0251	1	94	54.08	221.01	0.0251	1	94	57.14	235.17	0.0248	1	96	60.28	250.85
	1.25	0.0430	1	33	8.90	16.65	0.0424	1	34	9.08	17.06	0.0412	1	36	9.45	17.93	0.0407	1	37	9.82	19.20
	1.5	0.0701	1	11	3.13	3.51	0.0701	1	11	3.19	3.66	0.0676	1	12	3.31	3.77	0.0676	1	12	3.44	4.09
	2	0.0962	1	5	1.54	1.03	0.0962	1	5	1.56	1.07	0.0962	1	5	1.60	1.16	0.0962	1	5	1.65	1.25
0.15	0.25	0.1359	1	2	1.01	0.10	0.1359	1	2	1.01	0.11	0.1359	1	2	1.01	0.12	0.1359	1	2	1.01	0.13
	0.5	0.0843	1	7	3.18	4.41	0.0843	1	7	3.25	4.57	0.0843	1	7	3.39	4.91	0.0799	1	8	3.53	5.08
	0.75	0.0251	1	94	53.64	218.95	0.0251	1	94	55.14	225.91	0.0251	1	94	58.22	240.09	0.0248	1	96	61.38	255.84
	1.25	0.0424	1	34	9.07	17.01	0.0418	1	35	9.25	17.43	0.0412	1	36	9.62	18.65	0.0401	1	38	9.99	19.58
	1.5	0.0701	1	11	3.19	3.66	0.0701	1	11	3.25	3.82	0.0676	1	12	3.38	3.92	0.0676	1	12	3.50	4.25
	2	0.0962	1	5	1.56	1.08	0.0962	1	5	1.58	1.12	0.0962	1	5	1.63	1.21	0.0962	1	5	1.68	1.31
0.2	0.25	0.1359	1	2	1.01	0.11	0.1359	1	2	1.01	0.11	0.1359	1	2	1.01	0.12	0.1359	1	2	1.02	0.14
	0.5	0.0843	1	7	3.24	4.55	0.0843	1	7	3.30	4.71	0.0799	1	8	3.44	4.87	0.0799	1	8	3.58	5.23
	0.75	0.0251	1	94	55.11	225.79	0.0251	1	94	56.62	232.77	0.0248	1	96	59.70	248.17	0.0248	1	96	62.91	262.81
	1.25	0.0418	1	35	9.31	17.70	0.0412	1	36	9.50	18.13	0.0407	1	37	9.86	19.36	0.0396	1	39	10.24	20.30
	1.5	0.0676	1	12	3.28	3.69	0.0676	1	12	3.34	3.84	0.0676	1	12	3.47	4.15	0.0653	1	13	3.59	4.27
	2	0.0962	1	5	1.60	1.16	0.0962	1	5	1.62	1.20	0.0962	1	5	1.67	1.29	0.0962	1	5	1.72	1.39

Table 10. Phase-I and Phase-II datasets on the weight of scrap zinc alloy material in a die casting hot chamber process

	Phase-I			Phase-II		
i	$\bar{X}_i$	S_i	$\hat{\gamma}_i$	$\bar{X}_i$	S_i	$\hat{\gamma}_i$
1	292.6	2.701	0.0092	396.4	4.037	0.0102
2	289.0	0.707	0.0024	393.2	1.923	0.0049
3	291.4	2.073	0.0071	404.6	3.049	0.0075
4	288.0	3.937	0.0137	396.0	2.449	0.0062
5	290.0	0.707	0.0024	301.4	3.049	0.0101
6	288.2	1.303	0.0045	295.4	1.816	0.0061
7	535.4	8.264	0.0154	293.2	1.788	0.0061
8	518.4	7.224	0.0139	297.4	2.190	0.0074
9	529.2	9.203	0.0174	642.8	2.280	**0.0035***
10	527.0	9.591	0.0182	640.2	1.095	**0.0017**
11	533.6	4.929	0.0092	650.4	3.435	0.0053
12	439.2	3.114	0.0071	647.8	1.643	**0.0025**
13	447.2	2.774	0.0062	646.0	2.345	**0.0036**
14	443.4	8.173	0.0184	549.8	3.114	0.0057
15	434.0	2.549	0.0059	522.6	10.310	**0.0197**
16	436.0	1.224	0.0028	519.8	7.259	0.0140
17	437.6	2.408	0.0055	518.8	8.927	**0.0172**
18	419.6	4.037	0.0096	515.4	11.760	**0.0228**
19	422.4	4.159	0.0098	550.4	15.678	**0.0285**
20	416.8	3.962	0.0095	529.0	10.440	**0.0197**
21	420.4	4.979	0.0118	526.8	9.602	**0.0182**
22	421.6	2.302	0.0055	529.2	7.949	0.0150
23	418.4	4.393	0.0105	521.8	7.981	0.0153
24	410.4	4.219	0.0103	534.0	7.681	0.0144
25	449.0	6.204	0.0138	525.0	5.656	0.0108
26	441.6	3.781	0.0086	533.0	5.522	0.0104
27	393.2	6.220	0.0158	287.8	3.114	0.0108
28	401.8	1.483	0.0037	287.2	3.271	0.0114
29	412.6	3.049	0.0074	289.8	1.095	**0.0038**
30	461.4	7.700	0.0167	288.4	3.049	0.0106

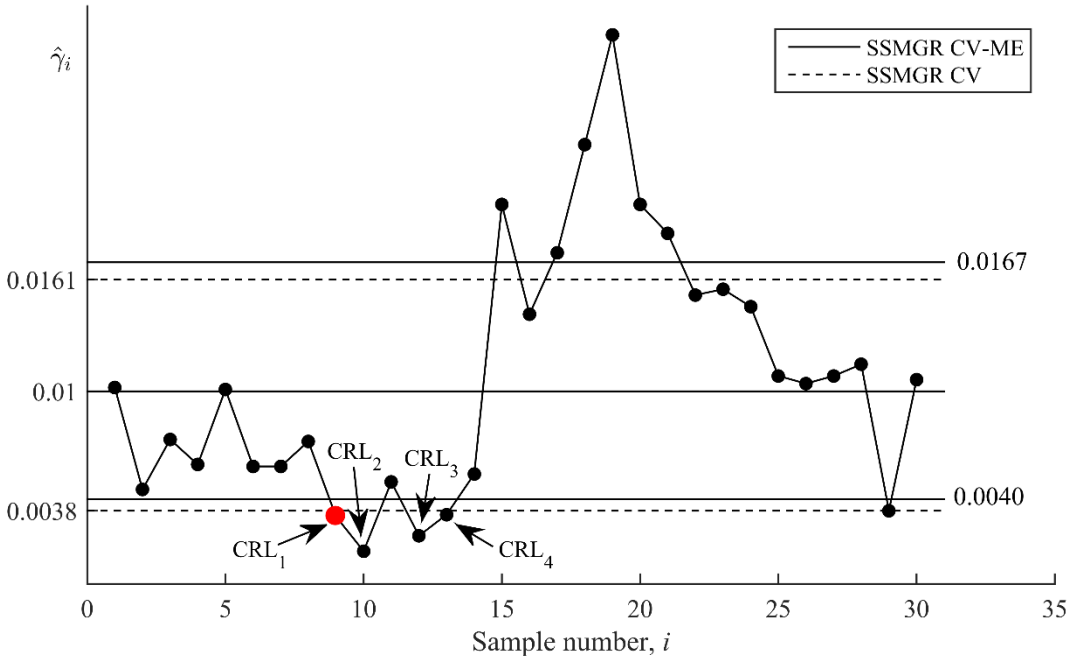

Figure 1. SSMGR CV and SSMGR CV-ME charts for monitoring the Phase-II sample CVs ($\hat{\gamma}_i$, for i = 1, 2, …, 30) on the weights of scrap zinc alloy material in a die casting hot chamber process